communications biology

A Nature Portfolio journal

Article

https://doi.org/10.1038/s42003-025-08775-5

Succinylation regulates boar sperm linear motility via reprogramming glucose metabolism

Qi Wang[1,5], Shanpeng Wang[1,5], Wenxian Zeng[2], Adedeji O. Adetunji[3], Lingjiang Min[1], Masayuki Shimada[4] & Zhendong Zhu[1]

Succinylation is a recently identified post-translational modification (PTM) that modulates enzyme activity and metabolism. However, how it regulates metabolic reprogramming in sperm remains unclear. In this study, we show that succinylation of pyruvate kinase M2 (PKM2) promotes oxidative phosphorylation (OXPHOS) and linear motility in boar sperm. Under low glucose (LG) extender, sperm linear motility was significantly enhanced, mitochondrial activity increased, glycolysis was inhibited, and the pentose phosphate pathway (PPP) was promoted. PKM2 interacted with voltage-dependent anion channel 3 (VDAC3), increasing mitochondrial permeability. Supplementing high glucose (HG) extender with succinic acid (SA) enhanced these effects. In contrast, the addition of resveratrol (RES) to LG extender, significantly reduced progressive motility (PM), decreased mitochondrial activity, and promoted the glycolysis pathway. Additionally, LG extender facilitated PKM2 succinylation and mitochondrial translocation. These findings demonstrate that PKM2 succinylation reprograms glucose metabolism from glycolysis to PPP, enhancing ATP production and supporting sustained linear motility, providing insights into optimizing sperm preservation.

Proper management of energy levels in mammalian sperm is crucial for maintaining their overall function. Following ejaculation, sperm exhibit stage-specific metabolic requirements as they traverse the female reproductive tract, undergo capacitation, and participate in fertilization[1]. These dynamic processes necessitate strategic adjustments in energy metabolism to optimize sperm function under varying physiological conditions. In mammalian sperm, ATP is primarily produced through glycolysis and oxidative phosphorylation (OXPHOS)[2,3]. ATP is a key energy source for maintaining sperm function, and sperm motility is closely linked to ATP production[4–6]. The precise coordination between glycolysis and mitochondrial OXPHOS exhibits significant interspecies variation in sperm energy metabolism[7,8]. Notably, boar sperm demonstrate a distinctive bioenergetic profile, with glycolysis serving as the predominant ATP source under basal physiological conditions[9]. However, mitochondrial function remains equally vital for maintaining boar fertility. Boar sperm rely heavily on OXPHOS and the activity of complex I to drive essential physiological processes[10]. Previous study has shown that reducing glucose level enhances boar sperm linear motility by modulating OXPHOS[11]. During sperm transport through the uterus, linear motility was the predominant mode of movement, improving sperm migration toward the oviduct. Notably, glucose levels in the boar's seminal plasma and the sow's uterine fluid were very low[12]. This physiological microenvironment may promote sperm OXPHOS, thereby facilitating the linear motility required for sperm transit through the female reproductive tract. After ovulation, the glucose content in the oviduct fluid increases significantly, enabling sperm capacitation and inducing circular motility. It is widely believed that the glycolysis pathway is essential for sperm hyperactivation[6]. Also, it has been reported that when HepG2 cells are cultured in a medium with HG levels, the glycolysis pathway is highly activated[13]. However, reducing glucose levels in the medium shuts down the glycolysis pathway and activates the OXPHOS pathway for ATP production in the cells[13]. Our previous study found that boar sperm exhibit different motility patterns under various substrate conditions, primarily due to changes in the balance of energy metabolism[14]. This process of metabolic pathway adjustment to adapt to varying energy demands of different environments is referred to as metabolic reprogramming[15].

Cellular metabolism is essential in shaping cell fate and function. Metabolic reprogramming orchestrates pleiotropic modulation of cellular activities[16], enabling cells to dynamically respond to physiological

[1]College of Animal Science and Technology, Qingdao Agricultural University, Qingdao, China. [2]School of Biological Science and Engineering, Shaanxi University of Technology, Hanzhong, China. [3]Department of Agriculture, University of Arkansas at Pine Bluff, Pine Bluff, AR, USA. [4]Laboratory of Reproductive Endocrinology, Graduate School of Integrated Sciences for Life, Hiroshima University, Hiroshima, Japan. [5]These authors contributed equally: Qi Wang, Shanpeng Wang.
e-mail: zzd2020@qau.edu.cn

fluctuations. It is well known that most cells generate ATP under normal conditions primarily through OXPHOS. However, in hypoxic environments, cells compensate for reduced OXPHOS activity by increasing the transcription of genes that encode glycolytic enzymes[17]. Resting T lymphocytes maintain cellular homeostasis primarily through OXPHOS, which efficiently generates ATP via mitochondrial electron transport chain activity. However, after antigen activation, the metabolic pathway in T cells shifts to glycolysis[18]. Numerous studies have shown that metabolic reprogramming can reshape epigenetic modifications, with many metabolites serving as substrates for post-translational modifications (PTMs)[11,18,19]. For example, the metabolites acetyl-CoA and S-adenosylmethionine participate in the initiation and progression of tumors through lysine acetylation and lysine methylation modifications[20,21]. Sperm, as highly differentiated cells, have inactive transcription and translation activities, primarily relying on PTMs to regulate their functions, making them an ideal model for investigating metabolic reprogramming. A recent study has found that the tricarboxylic acid (TCA) cycle intermediate itaconic acid acts as a metabolic regulator, mediating the reprogramming of boar sperm by shifting glucose flux from glycolysis to the pentose phosphate pathway (PPP), thereby enhancing NADPH production and supporting redox homeostasis[11].

SA is the key intermediate in the TCA, and functions as a critical metabolic regulator. A recent study demonstrated that succinylation of glycolytic enzymes plays a pivotal role in promoting tumor cell proliferation and cellular survival mode transitions[22]. Succinylation as a PTM, causes a more significant mass change (100 Da) compared to acetylation (40 Da) and methylation (14 Da)[23]. Traditionally, succinylation is regarded as a nonenzymatic reaction regulated by the concentration of succinyl-CoA in the mitochondria[24]. The TCA, glycolysis, ketogenesis, lipid, and amino acid metabolism are major sources of intracellular succinyl-CoA, indicating its crucial role in energy metabolism[25]. The dynamic balance of succinylation can be regulated by Sirt5. Although Sirt5 exhibits relatively weak deacetylase activity within the sirtuin family, it demonstrates effective removal of lysine succinylation[26,27], a characteristic that plays a vital role in maintaining energy homeostasis. RES is a promising activator of SIRT5[28,29]. Study show that RES increases SIRT5 de-succinylation activity without affecting its protein levels[30]. Succinylation influences cellular metabolic pathways by regulating the activity of metabolic enzymes. Pyruvate kinase (PK), a key enzyme in the glycolysis pathway, exists in multiple isoforms, with the M2 isoform (PKM2) dynamically transitioning between low-activity dimers and high-activity tetramers through allosteric regulation mediated by metabolic substrates[31,32]. A recent study has shown that under glucose starvation conditions, succinylation of PKM2 enhances mitochondrial energy metabolism, thereby supporting cell survival under nutritional depletion[22]. However, it is unclear if similar activity occurs in sperm under low glucose conditions.

Voltage-dependent anion Channel protein (VDAC) is a channel protein located on the outer mitochondrial membrane, allowing hydrophilic metabolites to pass through. Inside the cell, VDAC functions to balance OXPHOS and glycolysis to meet cellular energy demands[33]. A previous study shows that succinylation of PKM2 helps maintain mitochondrial function by stabilizing the protein levels of VDAC3. Therefore, we hypothesize that in low-glucose extender, the key glycolysis enzyme PKM2 in boar sperm undergoes succinylated, which blocks the glycolysis pathway and reprograms glucose metabolism from glycolysis to the PPP, with energy reliance shifting to OXPHOS. In this study, we found that PKM2 succinylation promotes its mitochondrial translocation, enhances mitochondrial activity, and reprograms glucose metabolism, thereby supporting sustained linear motility of sperm.

Results

Effects of different extenders on sperm motility and succinylation modification

Sperm were incubated with different extenders, and motility parameters were subsequently measured. The results showed that, in the HG extender, supplementation with various concentrations of SA did not affect total motility (TM) at lower concentrations (≤3 mM), but 4.5 mM SA significantly reduced sperm TM after 3 h (Fig. 1a, $p < 0.05$). Notably, compared to the control group, 3 mM SA improved sperm motility parameters, significantly increasing PM, curvilinear velocity (VCL), and average path velocity (VAP) (Fig. 1b, c and Supplementary Table 1, $p < 0.05$). However, it had no significant effect on linearity (LIN, VSL/VCL), straightness (STR, VSL/VAP), wobble coefficient (WOB, VAP/VCL), lateral amplitude (ALH) and beat-cross frequency (BCF) (Supplementary Table 1, $p > 0.05$). In contrast, in the LG group, 100 μM RES significantly decreased PM after 1 h of incubation (Fig. 1d–f and Supplementary Table 2, $p < 0.05$). Based on these motility parameters, 3 mM SA and 100 μM RES were selected for further experiments.

Comparative analysis of treatment groups (HG, LG, HG + SA, LG + RES) revealed no significant differences in TM across conditions (Table 1, $p > 0.05$). However, compared to the HG group, the LG group exhibited better motility parameters, with significantly higher PM, VSL, and VAP after both 1 and 3 h (Table 1, $p < 0.05$). When SA was added to the HG group, significant improvements in PM were observed after 3 h (Table 1, $p < 0.05$), whereas RES supplementation in the LG group significantly decreased PM, VSL, VCL, VAP, and WOB after 3 h (Table 1, $p < 0.05$). Moreover, during the incubation period, key indicators of hyperactivation, including amplitude of ALH and BCF, showed no significant differences among the treatment groups (Table 1 and Supplementary Fig. 1, $p > 0.05$), suggesting that no overt hyperactivation was induced under the tested conditions. The sperm motility trajectories differed after 1 h and 3 h of incubation in different extenders. The results showed that sperm in the HG extender exhibited circular motion, which intensified with prolonged incubation. In contrast, the low-dose group maintained a higher proportion of linear motility sperm. Notably, the addition of SA to the HG extender increased the linear motility subpopulations, whereas the supplementation of RES in the LG extender decreased the percentage of linear motility sperm (Fig. 1g).

Western blot results indicated that, compared to the LG group, the HG group showed significantly higher levels of sperm succinylation modification (Fig. 1h, i, $p < 0.05$). Furthermore, 3 mM SA further enhanced the levels of succinylation modification in the HG group (Fig. 1h, i, $p < 0.05$), while 100 μM RES inhibited succinylation modification under LG conditions (Fig. 1h, i, $p < 0.05$).

Effects of different extenders on PK activity and succinylation modification of PKM2 in boar sperm

Results indicated that PKM2 was expressed in boar sperm, predominantly located in the principal piece of the sperm tail (Fig. 2a and Supplementary Fig. 2). In the PK activity assay, we found that the PK activity in the HG group was significantly higher than in the fresh semen (FS) and LG groups (Fig. 2b, $p < 0.05$). The addition of SA to the HG extender (HG + SA) significantly reduced PK activity (Fig. 2b, $p < 0.05$). However, no significant difference in PK activity was observed between the HG + SA and LG extender groups (Fig. 2b, $p > 0.05$). After the addition of RES to the LG extender group, PK activity significantly increased (Fig. 2b, $p < 0.05$).

Immunoprecipitation experiment demonstrated that sperm incubated in LG extender exhibited significantly higher PKM2 succinylation levels compared to the HG extender (Fig. 2c, d, $p < 0.05$), while FS and HG groups demonstrated comparable succinylation modification levels (Fig. 2c, d, $p > 0.05$).

Reducing glucose concentration promotes mitochondrial translocation of PKM2

Immunofluorescence results showed that the localization of PKM2 in sperm changed upon incubation in high-glucose (HG) and low-glucose (LG) extenders (Fig. 3a, b and Supplementary Fig. 3a, b). Under LG extender, PKM2 underwent marked redistribution from its principal piece tail to mitochondrial localization. However, no significant translocation was observed under HG treatment (Fig. 3a, b). This differential localization pattern was validated through mitochondrial fractionation and Western

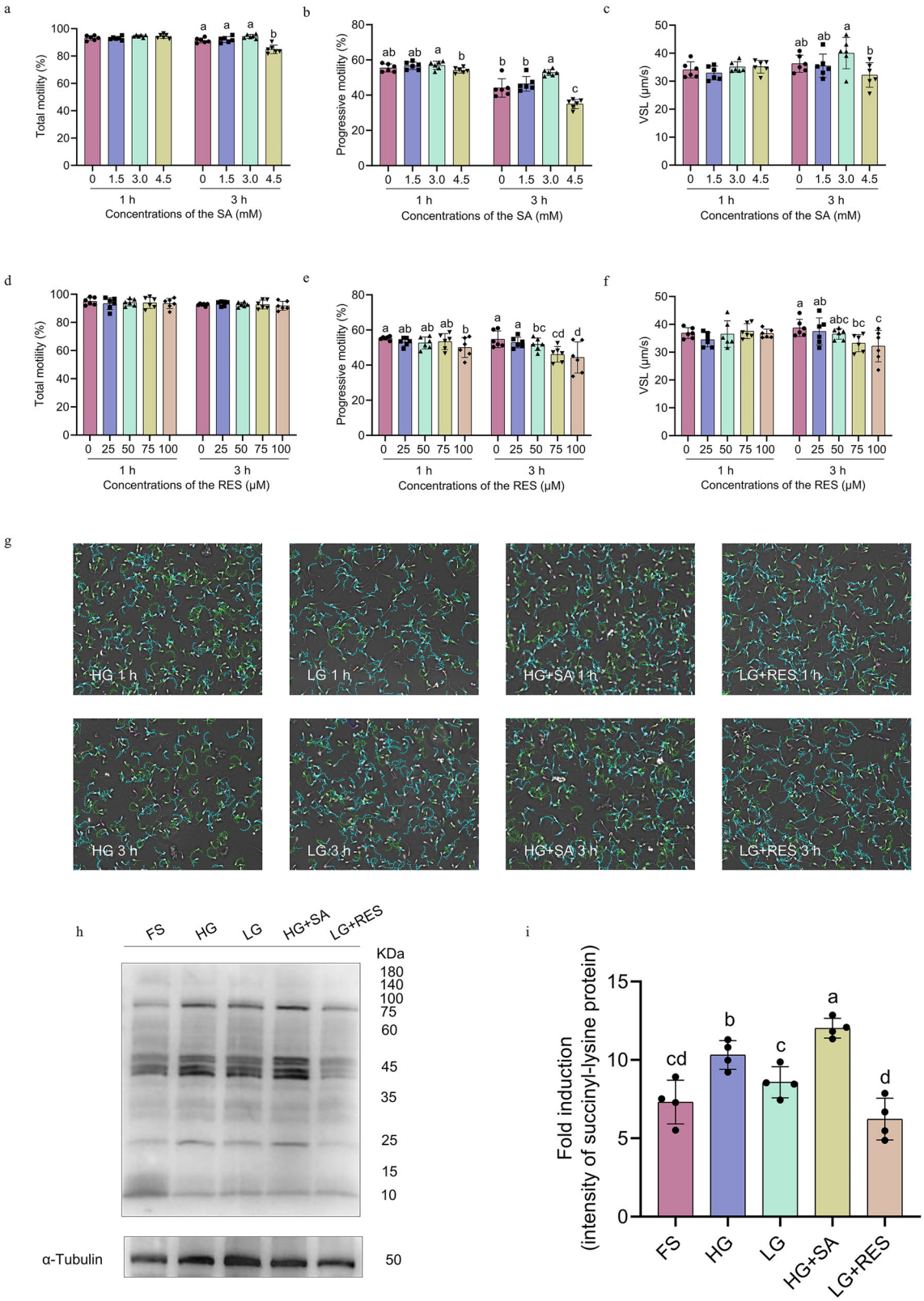

Fig. 1 | Effects of different extenders on sperm motility and succinylation modification. a–c Sperm were incubated with 0, 1.5, 3, and 4.5 mM SA in a HG extender for 1 h and 3 h. The sperm total motility (**a**), progressive motility (**b**), and VSL (**c**) were assessed using CASA. Data are presented as mean ± SD (n = 6). **d–f** Sperm were incubated with 0, 25, 50, 75, and 100 μM RES in an LG extender for 1 h and 3 h. The sperm total motility (**d**), progressive motility (**e**), and VSL (**f**) were assessed using CASA. Data are presented as mean ± SD (n = 6). **g** Sperm trajectories were recorded by CASA following 1 h and 3 h incubation under four extenders: HG extender, LG extender, HG + 3 mM SA, and LG + 100 μM RES. **h**, **i** Lysine succinylation levels in boar sperm proteins were evaluated after 3 h of treatment with FS, HG extender, LG extender, HG + 3 mM SA, and LG + 100 μM RES. Protein loading was normalized using an α-tubulin (**h**), and Western blot band intensities were quantified with ImageJ software (**i**). Data are expressed as mean ± SD (n = 4). [a-d:] Significant differences ($p < 0.05$) between treatments. FS fresh semen, HG high glucose, LG low glucose, RES resveratrol, SA succinic acid.

Table 1 | Effects of different extender on boar sperm motility parameters measured by CASA

	1 h				3 h			
	HG	LG	HG + SA	LG + RES	HG	LG	HG + SA	LG + RES
TM (%)	97.1 ± 1.1	96.5 ± 1.5	96.5 ± 1.5	95.4 ± 1.5	94.3 ± 1.3	95.3 ± 1.4	94.3 ± 1.8	95.3 ± 1.3
PM (%)	44.7 ± 2.1^{c}	60.3 ± 2.9^{a}	43.2 ± 3.2^{c}	54.8 ± 1.6^{b}	43.0 ± 1.6^{c}	56.8 ± 2.7^{a}	48.2 ± 1.7^{b}	48.1 ± 2.1^{b}
VCL (μm/s)	124.8 ± 11.1^{bc}	135.2 ± 4.1^{a}	117.4 ± 3.7^{c}	127.3 ± 7.1^{ab}	122.6 ± 6.8^{a}	131.3 ± 13.6^{a}	129.8 ± 7.5^{a}	108.5 ± 8.0^{b}
VSL (μm/s)	34.5 ± 5.1^{b}	40.5 ± 3.0^{a}	33.8 ± 4.6^{b}	35.3 ± 4.4^{ab}	34.5 ± 5.3^{b}	39.8 ± 1.2^{a}	37.0 ± 4.6^{ab}	33.3 ± 5.3^{b}
VAP (μm/s)	61.9 ± 7.2^{b}	69.5 ± 4.0^{a}	58.5 ± 1.1^{b}	61.9 ± 3.4^{b}	60.9 ± 4.0^{bc}	68.2 ± 7.2^{a}	64.0 ± 4.5^{ab}	54.4 ± 6.0^{c}
LIN (%)	28.3 ± 3.0	30.4 ± 1.9	29.2 ± 4.3	28.1 ± 3.4	28.3 ± 3.2	32.0 ± 1.9	28.7 ± 4.1	30.6 ± 3.4
STR (%)	55.8 ± 4.1	57.5 ± 2.3	57.7 ± 7.4	56.4 ± 5.1	55.9 ± 6.6	60.4 ± 3.7	56.9 ± 6.4	60.0 ± 4.9
WOB (%)	49.5 ± 2.2^{ab}	51.6 ± 2.2^{a}	49.7 ± 1.1^{ab}	48.5 ± 2.0^{b}	49.7 ± 1.2^{b}	52.1 ± 0.6^{a}	49.1 ± 2.7^{b}	49.6 ± 2.0^{b}
ALH (μm)	8.0 ± 0.6	8.1 ± 0.5	7.9 ± 0.6	8.0 ± 0.4	7.9 ± 0.7	7.6 ± 0.3	7.7 ± 0.3	7.5 ± 0.8
BCF (Hz)	36.7 ± 1.6	37.2 ± 4.8	36.7 ± 1.1	37 ± 4.5	37.7 ± 5.3	37.1 ± 0.8	37.2 ± 3.3	37.2 ± 2.2

Data are presented as mean ± SD (n = 6). $^{a-c}$: Significant differences ($p < 0.05$) between treatments.
TM total motility, *PM* progressive motility, *HG + SA* addition of succinic acid (3 mM) in HG extender, *LG + RES* addition of resveratrol (100 μM) in LG extender, *VCL* curvilinear velocity, *VSL* straight-line velocity, *VAP* average path velocity, *BCF* beat-cross frequency, *ALH* lateral amplitude, *STR* straightness (VSL/VAP), *LIN* linearity (VSL/VCL), *WOB* wobble (VAP/VCL).

blot analysis, which demonstrated a significant increase (Fig. 3c, d, $p < 0.05$) in mitochondrial PKM2 content in LG-treated sperm compared to the HG groups. Notably, in the fresh semen control samples, two distinct PKM2 immunoreactive bands of different sizes were observed.

Effect of different extenders on the glycolysis pathway in boar sperm

As shown in Fig. 4a–c, sperm incubated in LG extender for 3 h exhibited significantly lower lactate dehydrogenase (LDH) activity, phosphofructokinase (PFK) activity, and lactate levels compared to the HG group ($p < 0.05$). Notably, FS and the LG group showed no significant differences in LDH activity, and lactate levels (Fig. 4a, b, $p > 0.05$). After the addition of SA to the HG extender (HG + SA), LDH, lactate levels, and PFK activity levels were significantly lower compared to the HG extender group (Fig. 4a–c, $p < 0.05$). However, upon adding RES (LG + RES), the sperm's LDH activity, PFK activity, and lactate levels were significantly increased (Fig. 4a–c, $p < 0.05$).

Effect of different extenders on mitochondrial permeability and function in boar sperm

Western blot analysis confirmed the expression of voltage-dependent anion channel 3 (VDAC3) in boar sperm (Fig. 5a). As a critical regulator of mitochondrial outer membrane permeability, VDAC3 modulates metabolite transport, thereby influencing oxidative phosphorylation (OXPHOS) and cellular survival. Immunoprecipitation assays revealed significantly enhanced interaction between PKM2 and VDAC3 in sperm cultured under LG extender compared to the HG extender group (Fig. 5b, c, $p < 0.05$), while no significant difference was observed between the FS and HG groups (Fig. 5b, c, $p > 0.05$). Further analysis demonstrated that LG-cultured sperm displayed a significantly increased mitochondrial permeability transition pore (MPTP) opening relative to the HG group (Fig. 5d, e, $p < 0.05$). Supplementation of HG extender with SA significantly elevated MPTP opening (Fig. 5d, e, $p < 0.05$), whereas RES treatment in LG extender reduced MPTP opening (Fig. 5d, e, $p < 0.05$). Further mitochondrial functional assessments demonstrated that, compared to the HG extender, the LG extender significantly increased the proportion of sperm with high mitochondrial membrane potential (HMMP) (Fig. 5f, g and Supplementary Fig. 11, $p < 0.05$), as well as the activity of mitochondrial respiratory chain complex IV and ATP levels (Fig. 5h, i, $p < 0.05$). Additionally, SA treatment enhanced HMMP, mitochondrial respiratory chain complex IV activity, and ATP levels in the HG group, whereas RES treatment reduced these parameters in the LG group (Fig. 5f-i, $p < 0.05$).

Effect of different extenders on the pentose phosphate pathway in boar sperm

To elucidate the functional consequences of PKM2 succinylation on metabolic pathway switching between glycolysis and the pentose phosphate pathway (PPP), we quantitatively assessed NADPH levels and the activities of 6PGD and G6PD across experimental groups (Fig. 6). Comparative analysis revealed that sperm cultured in HG extender maintained significantly elevated NADPH levels compared to both FS and LG groups (Fig. 6a, $p < 0.05$). Notably, supplementation with SA in HG extender did not significantly alter NADPH concentrations relative to HG group (Fig. 6a, $p > 0.05$), while RES treatment in LG extender similarly showed no statistically significant effect on NADPH levels compared to LG group (Fig. 6a, $p > 0.05$). Additionally, sperm in the LG extender exhibited significantly higher 6PGD and G6PD activities than those in the FS and HG groups (Fig. 6b, c, $p < 0.05$). In the HG extender group, the addition of SA significantly increased the activities of 6PGD and G6PD (Fig. 6b, c, $p < 0.05$). Conversely, the addition of RES to the LG extender significantly reduced the activities of both 6PGD and G6PD (Fig. 6b, c, $p < 0.05$).

Discussion

Succinylation is a unique, relatively recently discovered, meagerly studied PTM[34,35], similar to hydroxylation, where the succinyl group couples with lysine residues of proteins[36]. This biochemical process is mediated by the metabolic intermediate succinyl-CoA, which is the donor for modifying specific lysine residues[23]. However, the regulation of succinylation in mature sperm remains poorly understood. Sperm are highly specialized cells with minimal transcriptional and translational activity, and thus rely heavily on PTMs to regulate their function. Notably, mature boar sperm retain functional mitochondria within the midpiece, which generate ATP through oxidative phosphorylation (OXPHOS) to support PM[11]. These mitochondria harbor key enzymes of the TCA cycle, including succinyl-CoA synthetase, which catalyzes the conversion of succinate into succinyl-CoA within the mitochondrial matrix[37]. Succinyl-CoA, as the succinyl group donor, is critical for driving non-enzymatic lysine succinylation, and its local availability directly influences the extent of succinylation[38]. Elevated levels of succinate can thus increase succinyl-CoA availability, promoting nonenzymatic lysine succinylation. Evidence suggests that succinate buildup is associated with increased protein succinylation across various cellular

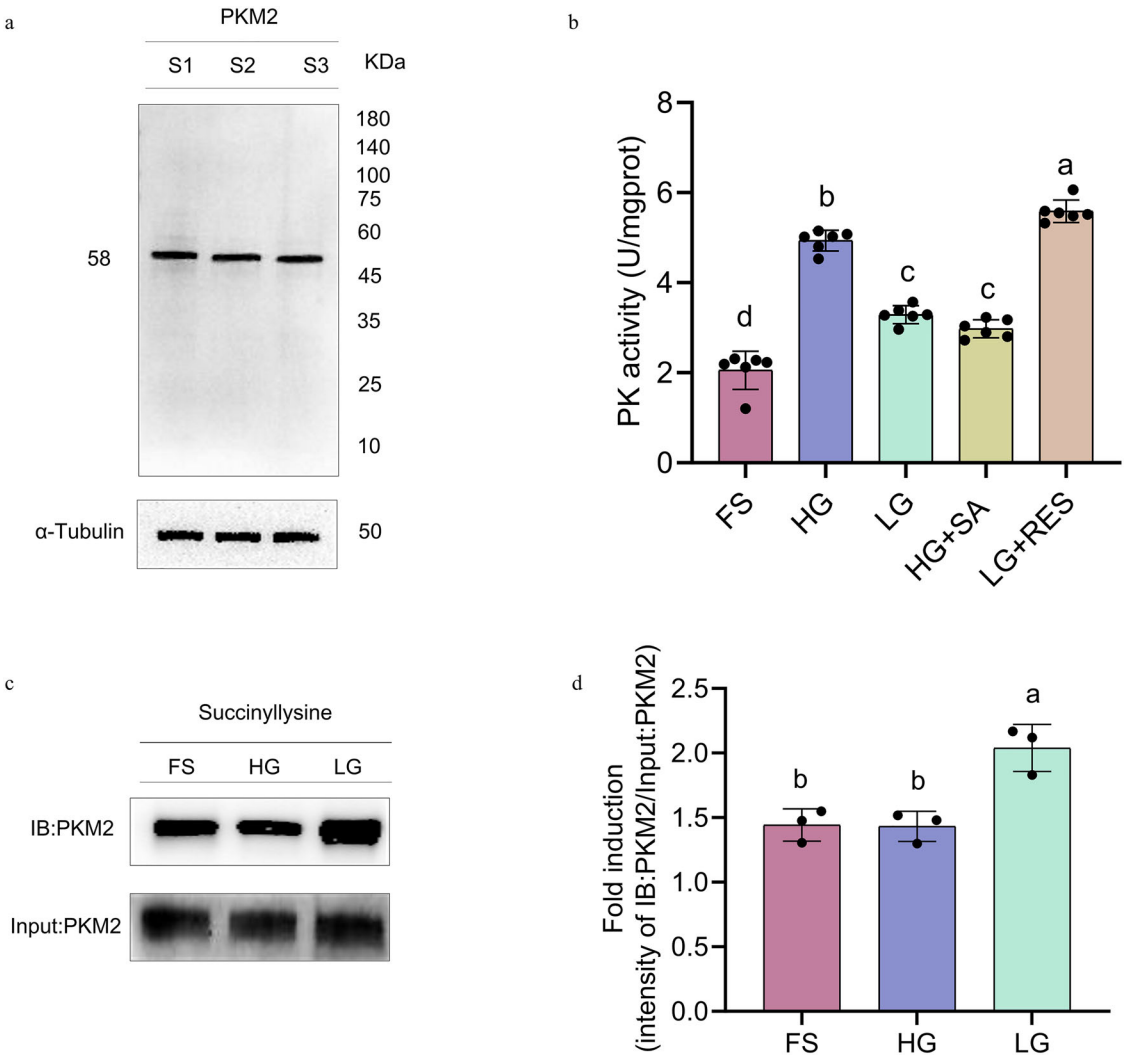

Fig. 2 | Effects of different extenders on PK activity and succinylation modification of PKM2 in boar sperm. a Western blotting of PKM2 in boar sperm. Protein loading was normalized using α-tubulin. **b** Boar sperm were treated with HG extender, LG extender, HG + 3 mM SA, or LG + 100 μM RES for 3 h to evaluate PK activity, compared with the control (FS). Data are expressed as mean ± SD (n = 6). Following 3 h of incubation with HG or LG extender, PKM2 protein bound to anti-succinylation antibody was immunoprecipitated from boar sperm lysates. Immunoprecipitated PKM2 was verified by Western blotting using a PKM2 antibody (**c**). Quantitative expression of precipitated PKM2 compared with the input generated from western blotting (**d**). Values represent mean ± SD (n = 3). [a-d]: Significant differences ($p < 0.05$) between treatments. FS fresh semen, HG high glucose, LG low glucose, RES resveratrol, SA succinic acid.

contexts[39–42]. In addition, the NAD⁺-dependent desuccinylase SIRT5 was reported to be expressed in mammalian sperm[43]. Our findings confirmed the presence of SIRT5 in mature boar sperm (Supplementary Fig. 4), and its activation by RES significantly reduced the boar sperm lysine succinylation levels, supporting its role in regulating PTM. In this study, we supplemented exogenous succinate to mimic intracellular accumulation and applied RES to reduce succinylation levels, thereby investigating the functional role of lysine succinylation in metabolic reprogramming and motility regulation of boar sperm.

Succinylation is an emerging area of importance in the functionality and diseases of central nervous system cells[44]. Current research has demonstrated that succinylation of PKM2 is a pivotal regulator of metabolic reprogramming[22]. In human colorectal cancer cells, succinylation at lysine K433 facilitates PKM2 mitochondrial translocation while modification at lysine K498 reduces enzymatic activity[22,45]. Our current findings demonstrate that PKM2 succinylation in boar sperm orchestrates a metabolic shift from glycolysis toward pentose phosphate pathway (PPP) activation and enhances oxidative phosphorylation (OXPHOS) activity. This metabolic reprogramming underlies the observed transition from circular to linear sperm motility patterns.

Sperm motility is dynamically regulated by metabolic pathways. In boar sperm, the ATP produced by mitochondrial OXPHOS is closely linked to linear motility[46]. CASA revealed distinct motility patterns in sperm incubated in different extenders. Sperm preserved in LG extender display higher linear motility and progressive viability, which correlate with increased mitochondrial activity and ATP levels. Lysine succinylation, a PTM prevalent in eukaryotic and prokaryotic cells[47], is critical in regulating sperm function. Notably, many proteins involved in glycolysis, the TCA cycle, fatty acid metabolism, and ketone body metabolism were targets of succinylation[44,48–50], highlighting its importance in metabolic regulation. Protein succinylation was emerged as a critical post-translational modification involved in metabolic regulation by modulating the activity of various metabolic enzymes[22,27,30]. Green et al. reported that the reduced activity of citrate synthase in hibernating ground squirrel skeletal muscle is mediated by decreased succinylation levels[51]. In mesenchymal stem cells, SIRT5 knockout leads to elevated global succinylation, which enhances glycolysis and the pentose phosphate pathway (PPP), ultimately promoting cell proliferation[52]. Additionally, decreased succinylation of myofibrillar proteins has been implicated in the pathogenesis of heart failure[53]. Comparative analysis of succinylation levels across treatment groups

demonstrated that high succinylation in HG extender correlated with circular motility and reduced PM, whereas low succinylation in LG extender promoted linear motility. The modulation of succinylation levels leads to opposing effects; increased succinylation enhances sperm linear motility and PM, while inhibition of succinylation reduces both linear and PM. This suggests that sperm can effectively regulate motility patterns by modulating the level of succinylation.

Increasing evidence shows succinylation regulates metabolic pathways by altering enzyme activity or stability. In asthenozoospermia, succinylation levels of enzymes related to energy metabolism and ATP generation in mitochondria are reduced, leading to a decline in sperm motility[54]. Additionally, increased lysine succinylation during buffalo sperm cryopreservation enhances mitochondrial lipid metabolism[55]. Pyruvate kinase (PK) was a rate-limiting enzyme in glycolysis with four isoforms, with PKM2 primarily expressed in embryos and cancer cells[56,57]. PKM2 can dynamically shift between dimer and tetramer forms, regulating enzyme activity[32,58]. Our results demonstrate that HG extender enhances PK activity compared to fresh semen. Interestingly, SA supplementation in HG extender further elevated succinylation and reduced PK activity, whereas RES in LG extender lowered succinylation and increased PK activity.

Immunofluorescence and Western blotting confirmed PKM2 expression in sperm, localized to the head and principal piece of the tail under physiological conditions. It is worth noting that site-specific succinylation may not parallel global succinylation patterns.

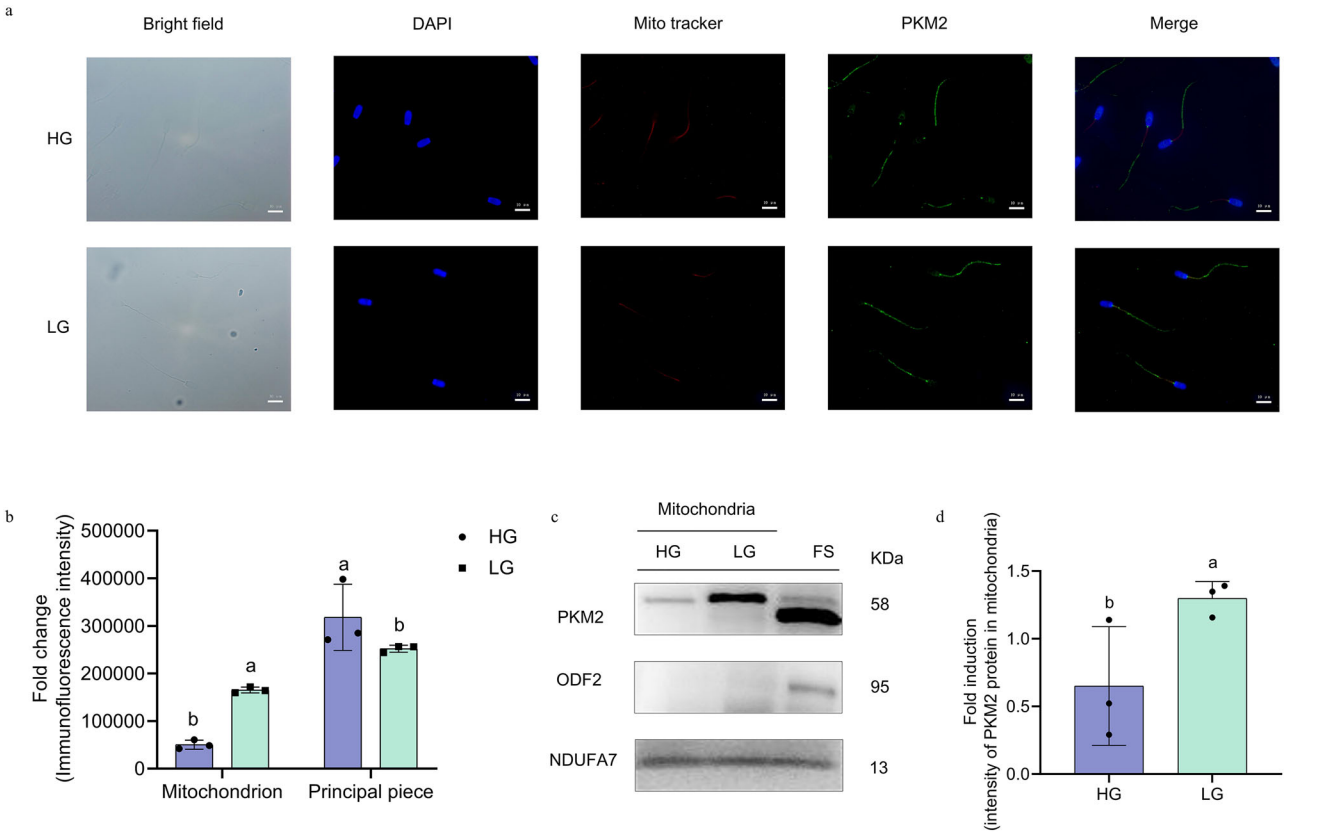

Fig. 3 | Reducing glucose concentration promotes mitochondrial translocation of PKM2. a, **b** After 3 h of incubation in HG or LG extenders, boar sperm were subjected to immunofluorescence analysis to evaluate subcellular localization. Mitochondria were identified with Mito Tracker™ Deep Red FM, nuclei were stained with Hoechst 33342. Immunofluorescence analysis of PKM2 in boar sperm. Bar = 10 μm (**a**). Quantitative data for immunofluorescence staining (**b**). Data are expressed as mean ± SD (n = 3). **c**, **d** After 3 h of incubation in HG or LG extenders, mitochondrial fractions were isolated from boar sperm for Western blot analysis. Western blotting of PKM2 in boar sperm mitochondria. Protein loading was normalized using an NDUFA7, and mitochondrial purity was validated with ODF2 (**c**), and Western blot band intensities were quantified with ImageJ software (**d**). Values represent mean ± SD (n = 3). [a, b]: Significant differences ($p < 0.05$) between treatments. FS fresh semen, HG high glucose, LG low glucose, RES resveratrol, SA succinic acid.

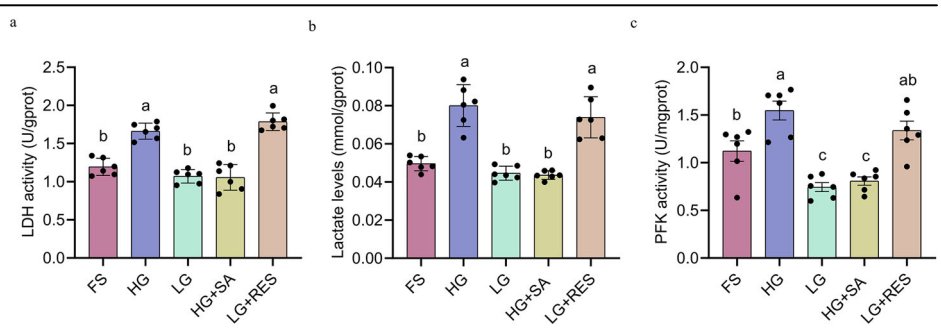

Fig. 4 | Effect of different extenders on the glycolysis pathway in boar sperm. Boar sperm were treated with HG extender, LG extender, HG + 3 mM SA, or LG + 100 μM RES for 3 h to evaluate LDH activity (**a**), lactate levels (**b**), and PFK activity (**c**), compared with the control (FS). Data are expressed as mean ± SD (n = 6). [a–c]: Significant differences ($p < 0.05$) between treatments. FS fresh semen, HG high glucose, LG low glucose, RES resveratrol, SA succinic acid, LDH lactate dehydrogenase, PFK phosphofructokinase.

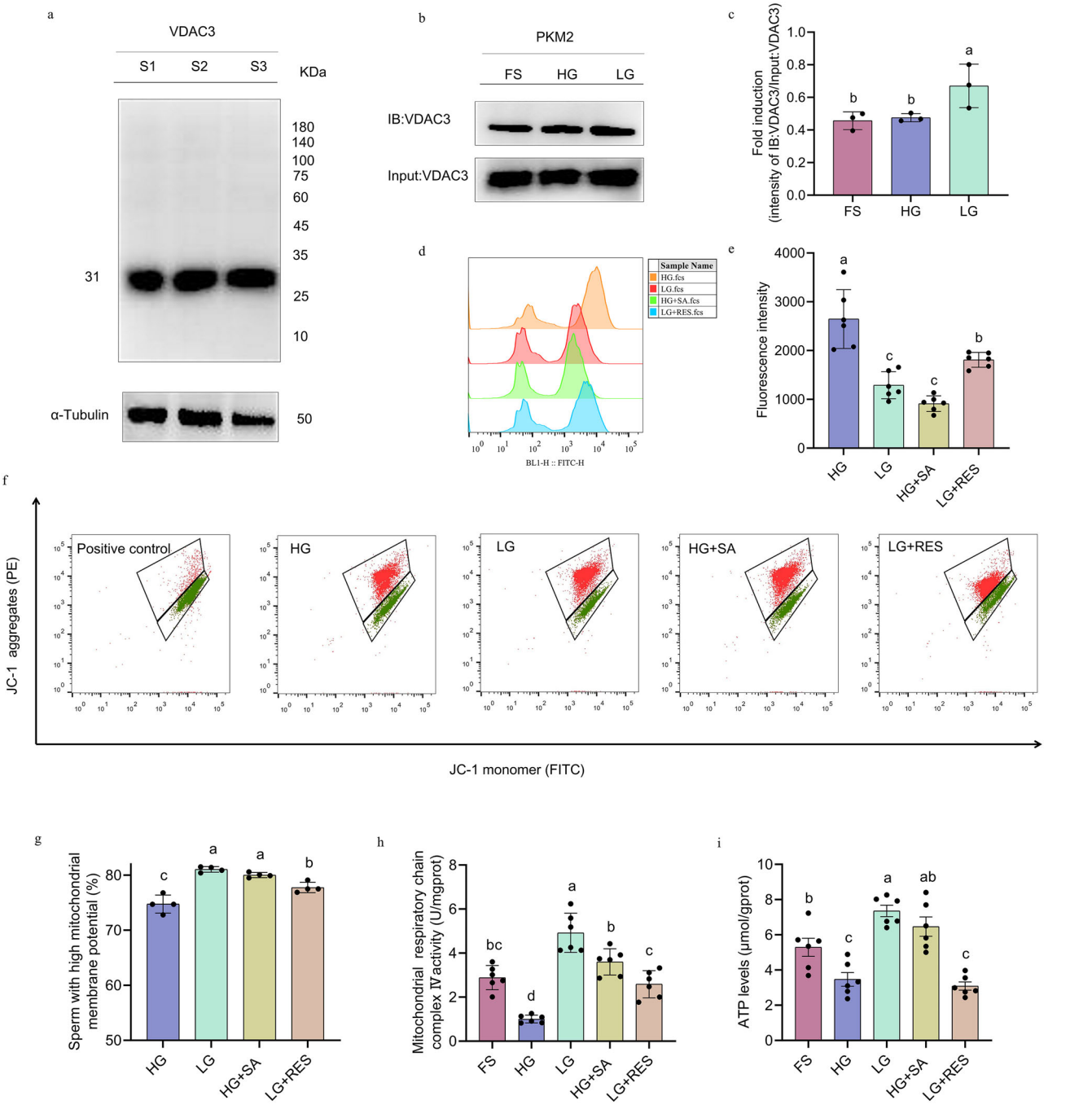

Fig. 5 | Effect of different extenders on mitochondrial permeability and function in boar sperm. a Western blotting of VDAC3 in boar sperm. Protein loading was normalized using α-tubulin. **b**, **c** Following 3 h of incubation with HG or LG extender, VDAC3 protein bound to anti-PKM2 antibody was immunoprecipitated from boar sperm lysates. Immunoprecipitated VDAC3 was verified by Western blotting using a VDAC3 antibody (**b**). Quantitative expression of precipitated VDAC3 compared with the input generated from western blotting (**c**). Data are expressed as mean ± SD (n = 3). **d**, **e** Following 3 h incubation with HG extender, LG extender, HG + 3 mM SA, or LG + 100 μM RES, mitochondrial membrane permeability was assessed by measuring the opening of the MPTP. Flow cytometric analysis of sperm mitochondrial permeability transition pore opening after 3 h of incubation was performed (**d**). The fluorescence intensity of stained sperm was analyzed, with higher fluorescence intensity indicating lower MPTP opening (**e**). Data are expressed as mean ± SD (n = 6). **f**, **g** After 3 h of treatment with HG extender, LG extender, HG + 3 mM SA, or LG + 100 μM RES, changes in sperm mitochondrial membrane potential were evaluated. Flow cytometric analysis of sperm mitochondrial membrane potential after 3 h of incubation was conducted (**f**), and the percentage of sperm with high mitochondrial membrane potential was determined (**g**). Data are expressed as mean ± SD (n = 4). Effects of HG extender, LG extender, HG + 3 mM SA, or LG + 100 μM RES treatment on sperm mitochondrial complex IV enzyme activity (**h**) and ATP levels were assessed after 3 h of incubation (**i**). Data are expressed as mean ± SD (n = 6). $^{a\text{-}c}$: Significant differences ($p < 0.05$) between treatments. FS fresh semen, HG high glucose, LG low glucose, RES resveratrol, SA succinic acid.

Immunoprecipitation assays revealed higher PKM2 succinylation in LG extender, contrasting with the overall lower global succinylation in LG extender sperm in the present study. In a study on diabetic retinopathy, both increased and decreased succinylation sites were identified across different proteins[59]. The elevated PKM2 succinylation observed under low-glucose conditions in this study may reflect increased local availability of succinyl-CoA within specific subcellular compartments. Unfortunately, we do not have data to reveal these phenomena, which is one of the limitations of the

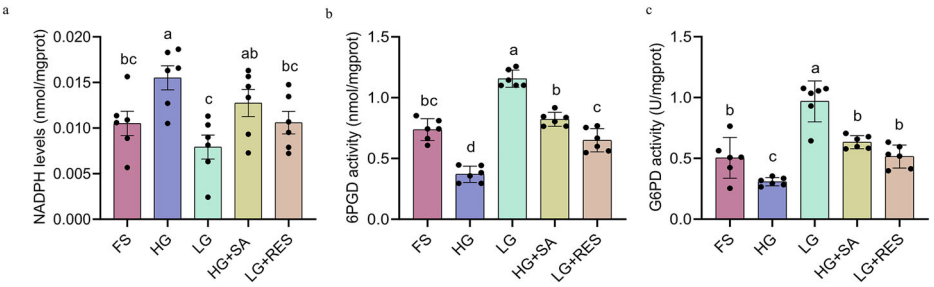

Fig. 6 | Effect of different extenders on pentose phosphate pathway in boar sperm. Boar sperm were treated with HG extender, LG extender, HG + 3 mM SA, or LG + 100 μM RES for 3 h to evaluate NADPH levels (**a**), 6PGD activity (**b**), and G6PD activity (**c**), compared with the control (FS). Data are expressed as mean ± SD (n = 6). [a-d]: Significant differences ($p < 0.05$) between treatments. FS fresh semen, HG high glucose, LG low glucose, RES resveratrol, SA succinic acid, NADPH nicotinamide adenine dinucleotide phosphate, 6PGD 6-phosphogluconate dehydrogenase, G6PD glucose-6-phosphate dehydrogenase.

present study. Therefore, further studies will be required to elucidate this concept in the future. This paradox may explain the reduced linear motility observed upon RES-mediated desuccinylation in LG extender. Prior study suggest that oxidative stress induces PKM2 mitochondrial translocation to stabilize Bcl-2 and inhibit apoptosis[60]. Our investigation of PKM2 subcellular localization demonstrated that HG extender sperm retained PKM2 in the principal piece of the tail, while LG extender triggered mitochondrial translocation, likely mediated by succinylation. This aligns with observations in glucose-deprived tumor cells[22]. Mitochondrial isolation and Western blotting further confirm that the mitochondrial PKM2 levels in LG extender sperm are significantly higher than in the HG extender group. Notably, two PKM2 molecular weight forms were detected in intact sperm, while only one form persisted in purified mitochondria, confirming succinylation-dependent translocation.

Cellular ATP production in mammals' sperm relies on glycolysis and OXPHOS, with pathway selection dictated by oxygen availability and substrate composition[2,3]. These systems cooperatively maintain energy homeostasis under fluctuating microenvironments[61]. Studies show that glycolysis inhibition restores OXPHOS functionality[62,63]. On this note, we hypothesize that PKM2 succinylation in sperm suppresses glycolysis, thereby enhancing OXPHOS to sustain ATP production. Our results show that sperm cultured in LG extender exhibit increased mitochondrial permeability, elevated complex IV activity, higher ATP levels, and enhanced mitochondrial membrane potential. In contrast, RES-mediated succinylation reduction impaired mitochondrial function. These findings underscore the role of succinylation in regulating mitochondrial activity. VDAC3, which regulates mitochondrial permeability, was critical for cell survival[22]. Enhanced PKM2 succinylation coincided with increased membrane permeability, suggesting a functional link. Immunoprecipitation confirmed stronger PKM2-VDAC3 interaction in LG extender, potentially maintaining mitochondrial ATP production by increasing mitochondrial permeability.

The PPP in sperm primarily functions to produce NADPH, which reduces oxidized glutathione to its reduced form, mitigating oxidative stress and maintaining cellular redox homeostasis[64]. Our previous results indicated that sperm incubated in LG extender produces a significant amount of ROS through mitochondrial OXPHOS[14]. In this study, sperm incubated in LG extender showed the opening of the mitochondrial permeability transition pore (MPTP), which alters intracellular Ca^{2+} homeostasis and releases ROS[65]. To counteract excessive ROS, cells must increase NADPH levels to neutralize ROS[66]. According to a precious study, lung adenocarcinoma cells activate NADPH synthesis by increasing G6PD transcription and translation to combat oxidative stress[67]. However, as specialized cells, sperm have limited transcriptional and translational activity, and they can respond to oxidative stress by enhancing the activity of PPP-related enzymes[11]. The branching point of PPP and glycolysis is glucose-6-phosphate (G6P) produced from glucose[68]. PPP activation is triggered by G6P accumulation when glycolysis is inhibited[66,69,70]. In this study, the inhibition of glycolysis may explain the upregulation of G6PD and 6PGD enzyme activity. NADPH levels decreased after 3 h of LG extender incubation, suggesting that sperm may neutralize ROS by consuming NADPH.

Nevertheless, this study has certain limitations due to inherent differences between in vivo and in vitro storage environments. The glucose concentrations used in our system (HG: 153 mM; LG: 30.6 mM) do not fully replicate the physiological glucose levels found in seminal plasma, uterine fluid, or oviductal fluid. However, such concentrations are commonly employed in in vitro sperm preservation studies. Similar to the use of non-physiological agents (e.g., caffeine or heparin) in in vitro capacitation models[71,72], modified Modena extenders can be used to simulate specific metabolic conditions. These in vitro models offer controlled metabolic environments for mechanistic investigations. Previous study shown that variations in extender composition can mimic key physiological transitions in sperm, including changes in motility patterns and metabolic state[14]. In this context, we designed HG and LG extenders to induce glycolysis- and OXPHOS-dominant states, respectively, thereby providing a tractable platform to investigate the regulatory role of succinylation in sperm metabolic programming and functional adaptation. The core mechanism revealed in this study—succinylation-mediated metabolic regulation in boar sperm—is likely to be conserved across mammals. Succinylation has also been identified in human and buffalo cells[22,55], suggesting potential cross-species relevance. However, given known species-specific differences in sperm metabolism and the use of an in vitro model, caution is warranted when extrapolating these findings to other species or in vivo conditions. Further research is needed to confirm the universality of these mechanisms.

In summary, as shown in Fig. 7, after ejaculation, PKM2 succinylation inhibits glycolysis activity and promotes mitochondrial translocation of PKM2, stabilizing OXPHOS to sustain linear motility during transit to the oviduct. Concurrent PPP activation maintains redox homeostasis. After ovulation, the elevated glucose concentration in the oviduct relieves the inhibition of PKM2 activity, reactivating glycolysis and promoting sperm hyperactivation for fertilization. This dynamic metabolic switching mechanism ensures sperm function adapts to the physiological microenvironment.

Methods

Ethical approval

We have complied with all relevant ethical regulations for animal use. All animal treatments and experimental procedures were approved by the Qingdao Agricultural University Institutional Animal Care and Use Committee (QAU-1121010).

Chemicals

Unless specified otherwise, routine chemicals and reagents were purchased from Sigma-Aldrich (Shanghai, China).

Semen collection and processing

Three healthy adult Duroc boars (aged 20.3 ± 3.5 months) from Jimo Runmin Co., Ltd. (Qingdao, China) were selected for this experiment. All boars were housed in individual crates with ad libitum access to water and

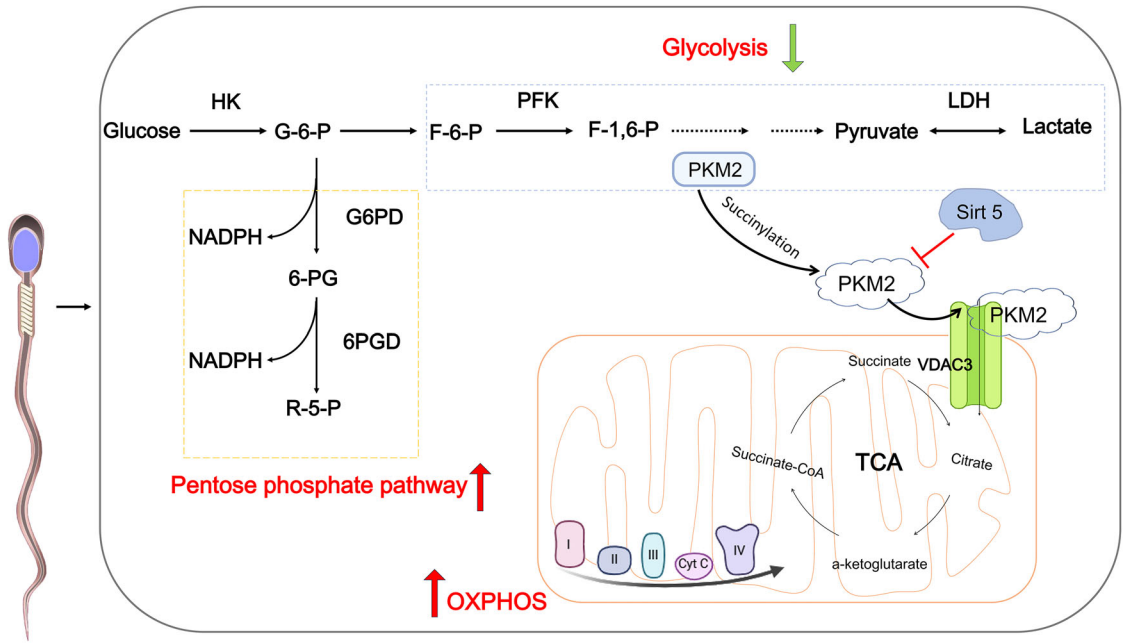

Fig. 7 | Mechanism by which succinylation induces glucose metabolic reprogramming to maintain linear motility in boar sperm. Succinylation of PKM2 reduces its enzymatic activity, inhibits the glycolysis pathway in sperm, and enhances enzymes activity involved in the NADPH-producing pentose phosphate pathway. The succinylation-mediated mitochondrial translocation of PKM2 in boar sperm increases mitochondrial permeability through interaction with VDAC3, thereby stimulating OXPHOS to generate ATP and sustain high linear sperm motility. Furthermore, Sirt5 modulates PKM2 succinylation levels through its desuccinylase activity to maintain an optimal equilibrium between glycolysis pathway and OXPHOS. G6PD Glucose-6-phosphate dehydrogenase, 6PGD 6-Phosphogluconate dehydrogenase, 6-PG: 6-Phosphogluconate, R-5-P Ribose-5-phosphate, NADPH Nicotinamide adenine dinucleotide phosphate (reduced form), F-6-P Fructose-6-phosphate, F-1,6-P Fructose-1,6-bisphosphate, HK Hexokinase, PFK Phosphofructokinase, LDH Lactate dehydrogenase, ETC Electron transport chain, Sirt5 sirtuin 5, OXPHOS oxidative phosphorylation, VDAC3 voltage-dependent anion Channel protein 3.

received a commercial diet. Semen was collected every five days with clean gloves and filtered with double gauze. To avoid individual differences, semen from each boar was pooled together for each collection. Each experimental replicate used a pooled semen sample. Thus, six replicates mean six experiments from six different pooled samples in this study. For evaluating boar sperm mitochondrial membrane potential and lysine succinylation levels, four replicates were performed. Immunofluorescence staining and immunoprecipitation detection were each performed with three replicates. In this study, only sperm with motility above 85% were selected for subsequent analysis.

Experimental design

According to our previous study[11], two Modena extenders were prepared: a HG extender containing 153 mM glucose and a LG extender containing 30.6 mM glucose. Previous study has shown that the enhancement of protein succinylation improved mitochondrial function[22]. To investigate the role of succinylation in boar sperm metabolic reprogramming and motility patterns, this study was based on the distinct metabolic characteristics of boar sperm under varying glucose concentrations. SA and RES were applied under HG and LG extenders. The pooled semen was divided into four equal portions and diluted with HG, LG, HG + SA, and LG + RES extenders, respectively, to achieve a final sperm concentration of 3.0×10^7 sperm/mL. The diluted sperm was incubated in a 37 °C water bath for up to 3 h. All semen samples from different treatment groups were assigned coded identifiers. Laboratory staff conducting sample handling and detection were blinded to group allocations and worked with anonymized samples. Based on pilot data, the mean difference of 15.2% between the groups, with a pooled standard deviation of 5.6%. Setting a two-sided significance level of 0.05 and a power of 0.8, the calculated sample size was approximately three biological replicates per group. The study design and analytical approach were documented internally and adhered to throughout the experimental process.

Evaluation of sperm motility

Sperm motility parameters were determined with the computer-assisted semen analysis (CASA) system (Hamilton Thorne Inc., Beverly, USA). According to our previous study[10], 5 μL of semen was mixed and placed onto a preheated Makler chamber, and preheated at 37 °C before use. More than three fields of view were selected for recording, and each process was independently repeated three times.

LDH activity determination

A lactate dehydrogenase assay kit (A020-2, Nanjing Jiancheng, Nanjing, China) was used to measure the lactate dehydrogenase (LDH) activity. According to our previous study[73], sperm samples were lysed by ultrasonication on ice, followed by centrifugation at 4000 × *g* for 5 min at 4 °C to collect the supernatant. The supernatant was mixed with the reaction reagents, and LDH activity was measured at 450 nm using a microplate reader.

Lactate levels determination

A lactate test kit (A019-2-1, Nanjing Jiancheng, Nanjing, China) was used to measure the lactate levels[73]. Briefly, sperm samples were lysed by ultrasonication on ice, followed by centrifugation at 4000 × *g* for 10 min at 4 °C to collect the supernatant. The mixtures of 1000 μL working solution, 200 μL chromogenic agent, and 20 μL supernatant for 10 min at 37 °C react accurately in a water bath. Thereafter, measurement was performed at 530 nm with a microplate reader.

PFK activity determination

Phosphofructokinase kit (A129-1-1, Nanjing Jianchen, Nanjing, China) was used to measure the activities of phosphofructokinase (PFK). As described by Chen et al. (2019)[74], sperm samples were centrifuged at 8000 × *g* for 10 min at 4 °C after ultrasonication on ice. The working solution was preheated for 10 min. The reaction mixture was prepared by combining 800 μL

of the working solution with 30 μL of cell supernatant. PFK activity was determined by continuously monitoring the NADH oxidation rate at 340 nm.

Immunofluorescence staining

As described by Howl et al.[75], sperm mitochondria were labeled with Mito Tracker™ Deep Red FM (1 μM) at 37 °C in the dark for 30 min. Following staining, the samples were washed twice with PBS and subsequently resuspended in fresh PBS. The stained sperm suspension was smeared onto glass slides and fixed with 4% paraformaldehyde for 10 min at room temperature, followed by three PBS washes. Samples were treated with PBS containing 3% (v/v) Triton X-100 for 60 min, then blocked with 10% (v/v) goat serum in PBS for 30 min to minimize nonspecific binding. The blocked samples were incubated with primary antibodies anti-PKM2 (A20991, AB clonal, Wuhan, China) for 2 h at 37 °C. Following primary antibody incubation, samples were treated with FITC-conjugated secondary antibodies for 30 min in the dark at 37 °C. Nuclear counterstaining was performed using Hoechst 33342[76]. Fluorescent signals were captured using a ZEISS DM2000 LED fluorescence microscope. All procedures were conducted in the dark to prevent fluorophore photobleaching.

PK activity determination

Pyruvate kinase Kit (BC0540, Solarbio, Beijing, China) was used to measure the activities of pyruvate kinase (PK). As described by Wang et al.[73], sperm samples were centrifuged at 8000 × *g* for 10 min at 4 °C after ultrasonication on ice. Then, the supernatant was collected to detect PK activity following the manufacturer's instructions. PK activity was quantified at 340 nm according to the manufacturer's protocol. The reaction mixture was incubated at 37 °C, with initial absorbance (A_1) recorded at 30 s and final absorbance (A_2) measured after 15 min. Enzyme activity was calculated from the NADH oxidation rate.

Extraction of sperm mitochondria

The sperm mitochondria were extracted using a mitochondrial extraction kit (SM0020, Solarbio, Beijing, China). As described by Bai et al.[77], sperm samples were resuspended in an ice-cold Lysis Buffer and subjected to homogenization 30 times using a glass homogenizer. The homogenate was centrifuged at 12,000 × *g* for 10 min at 4 °C to remove nuclei and unbroken sperm. The resulting supernatant was centrifuged again at 12,000 × *g* for 10 min at 4 °C to obtain highly purified mitochondria. Finally, the mitochondrial pellet was resuspended in 50 μL of Store Buffer and stored at −80 °C until further use.

Western blotting

According to our previous study[10], sperm protein extracts were prepared by ultrasonication on ice in 250 μL of ice-cold RIPA lysis buffer supplemented with 1% protease inhibitor cocktail, and centrifugation at 12,000 × *g* for 15 min at 4 °C. The protein samples were separated using SDS-PAGE on a 10% gel and transferred onto a polyvinylidene fluoride (PVDF) membrane. After blocking with 5% BSA in TBST for 2 h at room temperature. The membrane was incubated overnight at 4 °C with the primary antibody diluted in TBST containing 1% BSA, primary antibody including anti-succinyllysine (PTM-401, 1:1000, PTM BIO, Hangzhou, China), PKM2 (A20991, 1:1000 ABclonal, Wuhan, China), SIRT5 (bs-9456R, 1:1000, Bioss, Beijing, China), VDAC3 (bs-7647R, 1:2000, Bioss, Beijing, China), ODF2 (A3607, 1:500, ABclonal, Wuhan, China), NDUFA7 (A8441, 1:500, ABclonal, Wuhan, China) and α-Tubulin (ab7291, 1:10,000, Abcom, Shanghai, China). Following three 5 min TBST washes, membranes were incubated with HRP-conjugated secondary antibody (AS014, 1: 2000, ABclonal, Wuhan, China) diluted in TBST at room temperature for 1 h. Protein signals were detected using ECL Super (ED0015-A, Sparkjade, Jinan, China). Finally, visualization was performed using a gel imaging system (Alpha, Fluor Chem Q, Shanghai, China).

Immunoprecipitation

Total sperm protein was extracted using RIPA lysis buffer supplemented with 1% protease inhibitor cocktail. Anti-succinyllysine antibody (PTM-401, 1: 100, PTM BIO, Hangzhou, China) or anti-PKM2 antibody (A20991, 1:500, ABclonal, Wuhan, China) was directly added to whole sperm lysate and incubated overnight with agitation at 4 °C. Subsequently, IgG conjugated magnetic beads (8726 s, Cell Signaling Technology, Shanghai, China) were added and incubated for 3 h with agitation at 4 °C. Following incubation, the samples were centrifuged at 10,000 × *g* for 10 min at 4 °C, after which the supernatant was discarded and the bead-bound immunocomplexes were retained. Finally, the precipitated proteins were analyzed by Western blot using a 10% SDS-PAGE gel[11].

Mitochondrial respiratory chain complex IV activity determination

Mitochondrial complex IV activity of sperm was detected using a mitochondrial respiratory chain complex IV kit (BC0945, Solarbio, Beijing, China). According to our previous study[10], isolated sperm mitochondria were subjected to ultrasonication on ice. The enzymatic activity was quantified spectrophotometrically by monitoring the oxidation rate of reduced cytochrome c at 550 nm.

Sperm ATP levels determination

ATP levels of sperm was detected using an ATP assay kit (A095-1-1, Nanjing Jianchen, Nanjing, China). Sperm samples were homogenized in an ice bath. The resulting sperm suspension was subjected to a boiling water bath for 10 min. After heat treatment, experimental samples were incubated with working solution A, while control samples were treated with working solution B. Both sets of samples were incubated a 37 °C water bath for 30 min. Following incubation, a precipitation reagent was added to all samples, and the samples were centrifuged at 1500 × *g* for 5 min. The supernatant was collected and sequentially mixed with a color reagent and termination solution[10]. After incubation at 37 °C for 5 min, the absorbance was measured at 636 nm.

Mitochondrial permeability transition pore determination

Mitochondrial permeability transition pore assay kit (C2009S, Beyotime, Shanghai, China) was used to detect the mitochondrial permeability transition pore opening. As described by Qi et al.[22], sperm samples were incubated with the fluorescence quenching working solution at 37 °C for 30 min in the dark. Following incubation, the samples were centrifuged at 1000 × *g* for 5 min at room temperature to remove excess dye. The pelleted sperm samples were resuspended in the appropriate buffer for subsequent analysis. The fluorescence intensity of calcein was quantified by a flow cytometer (BeamCyte-1026M, BeamDiag, Changzhou, China). A total of 20,000 sperm events were analyzed.

Sperm mitochondrial membrane potential determination

Changes in sperm mitochondrial membrane potential were evaluated with the JC-1 Mitochondrial Membrane Potential Detection Kit (C2006S, Beyotime, Shanghai, China). As a positive control, sperm were preincubated with 10 μM CCCP for 30 min to induce depolarization. All sperm samples were incubated with JC-1 working solution at 37 °C in the dark for 30 min. Following incubation, the excess unincorporated dye was removed by two washes with ice-cold JC-1 assay buffer[10]. The stained sperm samples were evaluated by a flow cytometer. A total of 20,000 sperm events were analyzed.

Sperm NADPH levels determination

To measure Sperm NADPH levels, the Coenzyme II content test kit was used (A115-1-1, Nanjing Jianchen, Nanjing, China). As previously described by Cheng et al.[78], Alkaline extraction buffer was added to sperm suspensions, followed by ultrasonication on ice. The homogenates were heated in a boiling water bath for 5 min and centrifuged at 10,000 × *g* for 10 min at 4 °C. The resulting supernatant was transferred to fresh tubes and neutralized with an equal volume of acidic extraction buffer. After thorough

vortex mixing, samples were recentrifuged under identical conditions, and the final supernatant was immediately placed on ice for subsequent analysis. NADPH was used to reduce the oxidized form of 3-(4,5-dimethylthiazol-2-yl)-2,5-diphenyl tetrazolium bromide (MTT) to formazan. The NADPH content was determined by measuring the absorbance at 570 nm.

G6PD and 6PGD activity determination

A 6-glucose phosphate dehydrogenase Assay Kit (AK381U, Bioss, Beijing, China) and 6-phosphogluconate dehydrogenase Assay kit (AK123, Bioss, Beijing, China) were used to measure the activities of 6-glucose phosphate dehydrogenase (G6PD) and 6-phosphogluconate dehydrogenase (6PGD), Sperm samples were homogenized in ice-cold extraction buffer using ultrasonication on ice. The sperm homogenates were centrifuged at 8000 × *g* for 10 min at 4 °C to remove cellular debris, and the resulting supernatants were immediately placed on ice for subsequent analysis[11]. The enzymatic activities were determined by continuously monitoring the increase in absorbance at 340 nm.

Statistics and reproducibility

All experimental data were analyzed using IBM SPSS Statistics software (version 27; IBM Corp., Armonk, NY, USA). Before performing parametric testing, the normality of the distribution was assessed, and the homogeneity of variances was verified. The data were transformed by arcsine square root transformation when necessary. Intergroup comparisons were performed using either independent Student's t-tests for comparisons between two groups or one-way ANOVA with Tukey's post hoc test for multiple group comparisons. Data analysis was initially conducted using group codes, and group identities were unblinded only after statistical analysis and result interpretation were finalized. All ejaculates met the predefined inclusion criteria (≥85% motility) and were included in the analysis. No samples or data points were excluded after group allocation. All collected data were analyzed. All results are expressed as mean ± standard deviation. Graphs were created using GraphPad Prism 8.0 (GraphPad Software Inc., La Jolla, CA, USA). $p < 0.05$ was considered statistically significant.

Reporting summary

Further information on research design is available in the Nature Portfolio Reporting Summary linked to this article.

Data availability

The data presented in this study are available in the article. Supplementary Figs. 4–10 contain the original, unprocessed blot images that were used to create the graphs. The source data for all graphs are available in the Supplementary Data file.

Received: 3 April 2025; Accepted: 21 August 2025;
Published online: 30 August 2025

References

1. Pena, F. J. et al. An integrated overview on the regulation of sperm metabolism (glycolysis-Krebs cycle-oxidative phosphorylation). *Anim. Reprod. Sci.* **246**, 106805 (2022).
2. Gohil, V. M. et al. Nutrient-sensitized screening for drugs that shift energy metabolism from mitochondrial respiration to glycolysis. *Nat. Biotechnol.* **28**, 249–255 (2010).
3. Potter, M., Newport, E. & Morten, K. J. The Warburg effect: 80 years on. *Biochem. Soc. Trans.* **44**, 1499–1505 (2016).
4. Storey, B. T. Mammalian sperm metabolism: oxygen and sugar, friend and foe. *Int. J. Dev. Biol.* **52**, 427–437 (2008).
5. Mukai, C. & Travis, A. J. What sperm can teach us about energy production. *Reprod. Domest. Anim.* **47**, 164–169 (2012).
6. du Plessis, S. S., Agarwal, A., Mohanty, G. & van der Linde, M. Oxidative phosphorylation versus glycolysis: what fuel do spermatozoa use? *Asian J. Androl.* **17**, 230–235 (2015).
7. Marin, S. et al. Metabolic strategy of boar spermatozoa revealed by a metabolomic characterization. *FEBS Lett.* **554**, 342–346 (2003).
8. Mukai, C. & Okuno, M. Glycolysis plays a major role for adenosine triphosphate supplementation in mouse sperm flagellar movement. *Biol. Reprod.* **71**, 540–547 (2004).
9. Rodriguez-Gil, J. E. & Bonet, S. Current knowledge on boar sperm metabolism: comparison with other mammalian species. *Theriogenology* **85**, 4–11 (2016).
10. Wang, S. et al. 5-Aminolevulinate acid improves boar semen quality by enhancing the sperm mitochondrial function. *Theriogenology* **239**, 117389 (2025).
11. Zhu, Z. et al. Itaconate regulates the glycolysis/pentose phosphate pathway transition to maintain boar sperm linear motility by regulating redox homeostasis. *Free Radic. Biol. Med.***159**, 44–53 (2020).
12. Mateo-Otero, Y. et al. Metabolite profiling of pig seminal plasma identifies potential biomarkers for sperm resilience to liquid preservation. *Front. Cell Dev. Biol.* **9**, 669974 (2021).
13. Marroquin, L. D., Hynes, J., Dykens, J. A., Jamieson, J. D. & Will, Y. Circumventing the Crabtree effect: replacing media glucose with galactose increases susceptibility of HepG2 cells to mitochondrial toxicants. *Toxicol. Sci.* **97**, 539–547 (2007).
14. Zhu, Z. et al. Negative effects of ROS generated during linear sperm motility on gene expression and ATP generation in boar sperm mitochondria. *Free Radic. Biol. Med.* **141**, 159–171 (2019).
15. Losano, J. et al. Effect of mitochondrial uncoupling and glycolysis inhibition on ram sperm functionality. *Reprod. Domest. Anim.* **52**, 289–297 (2017).
16. Wu, H., Huang, H. & Zhao, Y. Interplay between metabolic reprogramming and post-translational modifications: from glycolysis to lactylation. *Front. Immunol.* **14**, 1211221 (2023).
17. Rodriguez-Enriquez, S. et al. Oxidative phosphorylation is impaired by prolonged hypoxia in breast and possibly in cervix carcinoma. *Int. J. Biochem. Cell Biol.* **42**, 1744–1751 (2010).
18. van der Windt, G. J. & Pearce, E. L. Metabolic switching and fuel choice during T-cell differentiation and memory development. *Immunol. Rev.* **249**, 27–42 (2012).
19. Nguyen, H. D. et al. Metabolic reprogramming of alloantigen-activated T cells after hematopoietic cell transplantation. *J. Clin. Investig.* **126**, 1337–1352 (2016).
20. Dancy, B. M. & Cole, P. A. Protein lysine acetylation by p300/CBP. *Chem. Rev.* **115**, 2419–2452 (2015).
21. Luo, M. Chemical and biochemical perspectives of protein lysine methylation. *Chem. Rev.* **118**, 6656–6705 (2018).
22. Qi, H. et al. Succinylation-dependent mitochondrial translocation of PKM2 promotes cell survival in response to nutritional stress. *Cell Death Dis.* **10**, 170 (2019).
23. Yang, Y. & Gibson, G. E. Succinylation Links Metabolism to Protein Functions. *Neurochem. Res.* **44**, 2346–2359 (2019).
24. Yang, L. et al. The growing landscape of succinylation links metabolism and heart disease. *Epigenomics* **13**, 319–333 (2021).
25. Carrico, C., Meyer, J. G., He, W., Gibson, B. W. & Verdin, E. The mitochondrial acylome emerges: proteomics, regulation by sirtuins, and metabolic and disease implications. *Cell Metab.* **27**, 497–512 (2018).
26. Colak, G. et al. Identification of lysine succinylation substrates and the succinylation regulatory enzyme CobB in *Escherichia coli*. *Mol. Cell Proteom.* **12**, 3509–3520 (2013).
27. Park, J. et al. SIRT5-mediated lysine desuccinylation impacts diverse metabolic pathways. *Mol. Cell* **50**, 919–930 (2013).
28. Gertz, M. et al. A molecular mechanism for direct sirtuin activation by resveratrol. *PLoS ONE* **7**, e49761 (2012).
29. Bagul, P. K., Dinda, A. K. & Banerjee, S. K. Effect of resveratrol on sirtuins expression and cardiac complications in diabetes. *Biochem. Biophys. Res. Commun.* **468**, 221–227 (2015).

30. Xiao, Z. P. et al. Sirtuin 5-mediated lysine desuccinylation protects mitochondrial metabolism following subarachnoid hemorrhage in mice. *Stroke* **52**, 4043–4053 (2021).
31. Rihan, M. & Sharma, S. S. Inhibition of Pyruvate kinase M2 (PKM2) by shikonin attenuates isoproterenol-induced acute myocardial infarction via reduction in inflammation, hypoxia, apoptosis, and fibrosis. *Naunyn Schmiedeb. Arch. Pharmacol.* https://doi.org/10.1007/s00210-023-02593-4 (2023).
32. Gui, D. Y., Lewis, C. A. & Vander Heiden, M. G. Allosteric regulation of PKM2 allows cellular adaptation to different physiological states. *Sci. Signal.* **6**, pe7 (2013).
33. Maldonado, E. N. & Lemasters, J. J. Warburg revisited: regulation of mitochondrial metabolism by voltage-dependent anion channels in cancer cells. *J. Pharm. Exp. Ther.* **342**, 637–641 (2012).
34. Tan, L. et al. Identification of lysine succinylome and acetylome in the vancomycin-intermediate *Staphylococcus aureus* XN108. *Microbiol. Spectr.* **10**, e0348122 (2022).
35. Peng, C. et al. The first identification of lysine malonylation substrates and its regulatory enzyme. *Mol. Cell Proteom.* **10**, M111 012658 (2011).
36. Zheng, S., Liu, Q., Liu, T. & Lu, X. Posttranslational modification of pyruvate kinase type M2 (PKM2): novel regulation of its biological roles to be further discovered. *J. Physiol. Biochem.* **77**, 355–363 (2021).
37. Huang, S., Wang, J. & Wang, L. Knockdown of Sucla2 decreases the viability of mouse spermatocytes by inducing apoptosis through injury of the mitochondrial function of cells. *Folia Histochem. Cytobiol.* **54**, 134–142 (2016).
38. Sreedhar, A., Wiese, E. K. & Hitosugi, T. Enzymatic and metabolic regulation of lysine succinylation. *Genes Dis.* **7**, 166–171 (2020).
39. Atamna, H. Heme, iron, and the mitochondrial decay of ageing. *Ageing Res. Rev.* **3**, 303–318 (2004).
40. Jiang, S. & Yan, W. Succinate in the cancer-immune cycle. *Cancer Lett.* **390**, 45–47 (2017).
41. Trauelsen, M. et al. Extracellular succinate hyperpolarizes M2 macrophages through SUCNR1/GPR91-mediated Gq signaling. *Cell Rep.* **35**, 109246 (2021).
42. Wu, J. Y. et al. Cancer-derived succinate promotes macrophage polarization and cancer metastasis via succinate receptor. *Mol. Cell* **77**, 213–227.e215 (2020).
43. Ali, M. A. et al. SIRT5 alleviates oxidative stress of boar sperm induced by cryopreservation through IDH2 and SOD2 pathway. *Theriogenology* **241**, 117424 (2025).
44. Gibson, G. E. et al. Alpha-ketoglutarate dehydrogenase complex-dependent succinylation of proteins in neurons and neuronal cell lines. *J. Neurochem.* **134**, 86–96 (2015).
45. Xiangyun, Y. et al. Desuccinylation of pyruvate kinase M2 by SIRT5 contributes to antioxidant response and tumor growth. *Oncotarget* **8**, 6984–6993 (2017).
46. Zhu, Z. et al. Gene expression and protein synthesis in mitochondria enhance the duration of high-speed linear motility in boar sperm. *Front. Physiol.* **10**, 252 (2019).
47. Chen, H. et al. Mild metabolic perturbations alter succinylation of mitochondrial proteins. *J. Neurosci. Res.* **95**, 2244–2252 (2017).
48. Smestad, J., Erber, L., Chen, Y. & Maher, L. J. 3rd Chromatin succinylation correlates with active gene expression and is perturbed by defective TCA cycle metabolism. *iScience* **2**, 63–75 (2018).
49. Hu, G. et al. Succinylation modified ovalbumin: structural, interfacial, and functional properties. *Foods* **11**, https://doi.org/10.3390/foods11182724 (2022).
50. Zhang, Y. et al. Lysine desuccinylase SIRT5 binds to cardiolipin and regulates the electron transport chain. *J. Biol. Chem.* **292**, 10239–10249 (2017).
51. Green, S. R. & Storey, K. B. Skeletal muscle of torpid Richardson's ground squirrels (Urocitellus richardsonii) exhibits a less active form of citrate synthase associated with lowered lysine succinylation. *Cryobiology* **101**, 28–37 (2021).
52. Ou, T. et al. SIRT5 deficiency enhances the proliferative and therapeutic capacities of adipose-derived mesenchymal stem cells via metabolic switching. *Clin. Transl. Med.* **10**, e172 (2020).
53. Ali, H. R. et al. Defining decreased protein succinylation of failing human cardiac myofibrils in ischemic cardiomyopathy. *J. Mol. Cell Cardiol.* **138**, 304–317 (2020).
54. Tian, Y. et al. Global proteomic analyses of lysine acetylation, malonylation, succinylation, and crotonylation in human sperm reveal their involvement in male fertility. *J. Proteom.* **303**, 105213 (2024).
55. Luo, X. et al. The freezability of Mediterranean buffalo sperm is associated with lysine succinylation and lipid metabolism. *FASEB J.* **36**, e22635 (2022).
56. Rihan, M. & Sharma, S. S. Inhibition of Pyruvate kinase M2 (PKM2) by shikonin attenuates isoproterenol-induced acute myocardial infarction via reduction in inflammation, hypoxia, apoptosis, and fibrosis. *Naunyn Schmiedeb. Arch. Pharmacol.* **397**, 145–159 (2024).
57. Christofk, H. R. et al. The M2 splice isoform of pyruvate kinase is important for cancer metabolism and tumour growth. *Nature* **452**, 230–233 (2008).
58. Wang, F. et al. SIRT5 desuccinylates and activates pyruvate kinase M2 to block macrophage IL-1beta production and to prevent DSS-induced colitis in mice. *Cell Rep.* **19**, 2331–2344 (2017).
59. Zhang, Y. et al. Sirt5-mediated desuccinylation of OPTN protects retinal ganglion cells from autophagic flux blockade in diabetic retinopathy. *Cell Death Discov.* **8**, 63 (2022).
60. Liang, J. et al. Mitochondrial PKM2 regulates oxidative stress-induced apoptosis by stabilizing Bcl2. *Cell Res.* **27**, 329–351 (2017).
61. Zheng, J. Energy metabolism of cancer: glycolysis versus oxidative phosphorylation (Review). *Oncol. Lett.* **4**, 1151–1157 (2012).
62. Fantin, V. R., St-Pierre, J. & Leder, P. Attenuation of LDH-A expression uncovers a link between glycolysis, mitochondrial physiology, and tumor maintenance. *Cancer Cell* **9**, 425–434 (2006).
63. Smolkova, K. et al. Waves of gene regulation suppress and then restore oxidative phosphorylation in cancer cells. *Int. J. Biochem. Cell Biol.* **43**, 950–968 (2011).
64. Pena, F. J. et al. Redox regulation and glucose metabolism in the stallion spermatozoa. *Antioxidants* **14**, https://doi.org/10.3390/antiox14020225 (2025).
65. Bravo, A., Sanchez, R., Zambrano, F. & Uribe, P. Exogenous oxidative stress in human spermatozoa induces opening of the mitochondrial permeability transition pore: effect on mitochondrial function, sperm motility and induction of cell death. *Antioxidants* **13**, https://doi.org/10.3390/antiox13060739 (2024).
66. Kuehne, A. et al. Acute activation of oxidative pentose phosphate pathway as first-line response to oxidative stress in human skin cells. *Mol. Cell* **59**, 359–371 (2015).
67. Polimeni, M. et al. Modulation of doxorubicin resistance by the glucose-6-phosphate dehydrogenase activity. *Biochem. J.* **439**, 141–149 (2011).
68. Jiang, P., Du, W. & Wu, M. Regulation of the pentose phosphate pathway in cancer. *Protein Cell* **5**, 592–602 (2014).
69. Qin, W. et al. S-glycosylation-based cysteine profiling reveals regulation of glycolysis by itaconate. *Nat. Chem. Biol.* **15**, 983–991 (2019).
70. Ozer, N., Aksoy, Y. & Ogus, I. H. Kinetic properties of human placental glucose-6-phosphate dehydrogenase. *Int. J. Biochem. Cell Biol.* **33**, 221–226 (2001).
71. Parrish, J. J. Bovine in vitro fertilization: in vitro oocyte maturation and sperm capacitation with heparin. *Theriogenology* **81**, 67–73 (2014).
72. Alminana, C. et al. Adjustments in IVF system for individual boars: value of additives and time of sperm-oocyte co-incubation. *Theriogenology* **64**, 1783–1796 (2005).

73. Wang, S. et al. Vibration emissions reduce boar sperm quality via disrupting its metabolism. *Biology* **13**, https://doi.org/10.3390/biology13060370 (2024).
74. Chen, L. et al. Effects of protein phosphorylation on glycolysis through the regulation of enzyme activity in ovine muscle. *Food Chem.* **293**, 537–544 (2019).
75. Howl, J., Silva, J. V., Fardilha, M. & Jones, S. *Cell Penetrating Peptides: Methods and Protocols* (ed. Ülo Langel) 293–306 (Springer, 2022).
76. Zhang, W. et al. Beneficial effect of proline supplementation on goat spermatozoa quality during cryopreservation. *Animals* **12**, https://doi.org/10.3390/ani12192626 (2022).
77. Bai, K. et al. Supplementation of dimethylglycine sodium salt in sow milk reverses skeletal muscle redox status imbalance and mitochondrial dysfunction of intrauterine growth restriction newborns. *Antioxidants* **11**, https://doi.org/10.3390/antiox11081550 (2022).
78. Cheng, J. et al. G6PD lactylation is involved in regulating redox balance of boar sperm in low glucose extender. *Theriogenology* **239**, 117388 (2025).

Acknowledgements

This work was supported in part by National Natural Science Foundation (32272884 and 32102545), the Shandong Provincial Natural Science Foundation (ZR2024QC066), the Shandong Province Higher Educational Program for Young Innovation Talents (2022KJ170), the Start-up Fund for High-level Talents of Qingdao Agricultural University (1121010).

Author contributions

Qi Wang: Writing-original draft, Investigation, Data curation. Shanpeng Wang: Validation, Methodology, Data curation. Lingjiang Min and Masayuki Shimada: Formal analysis, Conceptualization. Wenxian Zeng: Formal analysis, Conceptualization. Adedeji O. Adetunji: Writing-review & editing. Zhendong Zhu: Writing-review & editing, Supervision, Project administration, Funding acquisition.

Competing interests

The authors declare no competing interests.

Additional information

Supplementary information The online version contains supplementary material available at https://doi.org/10.1038/s42003-025-08775-5.

Correspondence and requests for materials should be addressed to Zhendong Zhu.

Peer review information *Communications Biology* thanks the anonymous reviewers for their contribution to the peer review of this work. Primary handling editors: Frank Avila and Joao Valente.